

# Development of stabilized dual growth factor-loaded hyaluronate collagen dressing matrix

Journal of Tissue Engineering  
Volume 12: 1–13  
© The Author(s) 2021  
Article reuse guidelines:  
sagepub.com/journals-permissions  
DOI: 10.1177/2041731421999750  
journals.sagepub.com/home/tej



Jihyun Kim<sup>1,2\*</sup>, Kyoung-Mi Lee<sup>1,3\*</sup>, Seung Hwan Han<sup>4</sup>, Eun Ae Ko<sup>1</sup>,  
Dong Suk Yoon<sup>1</sup>, Ik Kyu Park<sup>5</sup>, Hang-Cheol Shin<sup>6</sup>, Kwang Hwan Park<sup>1</sup>   
and Jin Woo Lee<sup>1,2,3</sup>

## Abstract

Patients with diabetes experience impaired growth factor production such as epidermal growth factor (EGF) and basic fibroblast growth factor (bFGF), and they are reportedly involved in wound healing processes. Here, we report dual growth factor-loaded hyaluronate collagen dressing (Dual-HCD) matrix, using different ratios of the concentration of stabilized growth factors—stabilized-EGF (S-EGF) and stabilized-bFGF (S-bFGF). At first, the optimal concentration ratio of S-EGF to S-bFGF in the Dual-HCD matrix is determined to be 1:2 in type I diabetic mice. This Dual-HCD matrix does not cause cytotoxicity and can be used *in vivo*. The wound-healing effect of this matrix is confirmed in type II diabetic mice. Dual HCD enhances angiogenesis which promotes wound healing and thus, it shows a significantly greater synergistic effect than the HCD matrix loaded with a single growth factor. Overall, we conclude that the Dual-HCD matrix represents an effective therapeutic agent for impaired diabetic wound healing.

## Keywords

Impaired wound healing, stabilized growth factor, epidermal growth factor, basic fibroblast growth factor, dual-hyaluronate collagen dressing matrix

Date received: 13 February 2021; accepted: 13 February 2021

## Introduction

Diabetes mellitus is categorized as a metabolic disease that is prevalent worldwide. The occurrence of diabetes is absent or rare only in few traditional communities.<sup>1,2</sup> Diabetes is characterized by the dysregulation of blood glucose level and progressive loss of pancreatic beta cells. Type I diabetes is associated with beta cell dysfunction, which in turn leads to insulin deficiency.<sup>3,4</sup> In contrast, type II diabetes is characterized by dysregulation of carbohydrates and progressive loss of beta cells, resulting in insulin resistance.<sup>5</sup> Diabetes mellitus has a deleterious effect on tissue healing, and therefore, impaired wound healing eventually occurs in individuals with diabetes.<sup>6</sup>

Generally, the process of wound healing involves hemostasis, inflammation, granulation and angiogenesis, re-epithelialization, and remodeling phases.<sup>4,7–9</sup> Specifically, the granulation and angiogenesis phase is downregulated in diabetic ulcers, leading to limited tissue

<sup>1</sup>Department of Orthopaedic Surgery, Yonsei University College of Medicine, Seoul, South Korea

<sup>2</sup>Brain Korea 21 PLUS Project for Medical Sciences, Yonsei University College of Medicine, Seoul, South Korea

<sup>3</sup>Severance Biomedical Science Institute, Yonsei University College of Medicine, Seoul, South Korea

<sup>4</sup>Department of Orthopaedic Surgery, Yonsei University College of Medicine, Gangnam Severance Hospital, Seoul, South Korea

<sup>5</sup>R&D Center, Genewel Co., Ltd., Sunnam, South Korea

<sup>6</sup>School of Systems Biomedical Science, Soongsil University, Seoul, South Korea

\*These authors contributed equally to this work.

## Corresponding authors:

Jin Woo Lee, Department of Orthopaedic Surgery, Yonsei University College of Medicine, 50-1, yonsei-ro, Seodaemun-gu, Seoul 03722, South Korea.  
Email: LJWOS@yuhs.ac

Kwang Hwan Park, Department of Orthopaedic Surgery, Yonsei University College of Medicine, 50-1, yonsei-ro, seodaemun-gu, Seoul 03722, South Korea.  
Email: KHPARK@yuhs.ac



remodeling. Growth factors play a pivotal role, as therapeutic agents, in impaired wound healing.<sup>10–12</sup> Recently, several studies have demonstrated the crucial role of growth factors such as epidermal growth factor (EGF), basic fibroblast growth factor (bFGF), and platelet-derived growth factor (PDGF) in promoting tissue repair.<sup>13–15</sup> These growth factors are secreted during the wound healing process from activated keratinocytes, endothelial cells, fibroblasts, macrophages, and platelets that help accelerate the healing process.<sup>16,17</sup> However, individuals with diabetes show impaired production of these growth factors.<sup>18–20</sup> In particular, EGF and bFGF are dysregulated during diabetic wound healing.<sup>21,22</sup> EGF enhances extracellular matrix (ECM) formation by stimulating proliferation and migration of keratinocytes,<sup>23,24</sup> while bFGF plays a major role in proliferation and differentiation of fibroblasts, angiogenesis of vascular smooth muscle cells, and wound repair.<sup>25,26</sup> Therefore, dysregulated growth factors result in delayed wound healing.

Although growth factors are potential therapeutic agents for the treatment of delayed wound healing associated with diabetes, they are of limited use *in vivo*. Growth factors are rendered inactive when applied onto the matrix, owing to their short half-life and instability at room temperature.<sup>27</sup> In our previous study, we developed a hyaluronate-collagen dressing (HCD) matrix that is suitable for base material. This HCD matrix helps retain moisture around the wound site, reduce pain, and exhibit hemostatic effects.<sup>28</sup> Additionally, in our previous study, we successfully established structurally stabilized growth factors and confirmed that structurally stabilized-EGF (S-EGF) and bFGF (S-bFGF) alone accelerate the wound healing process in type I and II diabetic mice.<sup>29</sup> Generally, the expression of most cytokines and chemokines, such as vascular endothelial growth factor (VEGF), bFGF, tumor necrosis factor- $\alpha$  (TNF- $\alpha$ ), interleukin 6 (IL-6), CC chemokine family, and high-mobility group box 1 (HMGB1), is down-regulated in both humans and mice with diabetes.<sup>30–32</sup> Among these cytokines, HMGB1 has been identified to be involved in the process of tissue repair and inflammatory response.<sup>33,34</sup> HMGB1 enhances angiogenesis through the regulation of VEGF in diabetic mice.<sup>35</sup> Furthermore, HMGB1 increases the expression of C-X-C chemokine 8 (CXCL8) and chemokine C-C ligand (CCL2), which recruit endothelial progenitor cells.<sup>36,37</sup> Promoted wound healing is also observed in diabetic mice by increasing re-epithelialization and human fibroblasts migration upon recombinant protein HMGB1 treatment.<sup>32</sup> Several studies have reported that the topical application of HMGB1 accelerates wound healing, while the inhibition of HMGB1 delays wound healing.<sup>7,32,35,38,39</sup> The ability of HMGB1 to promote tissue repair suggests its potential role in wound healing.

This study aimed to investigate the efficacy of dual growth factor-loaded HCD (Dual-HCD) matrix, stabilized

growth factors-stabilized-EGF (S-EGF) and stabilized-bFGF (S-bFGF) loaded HCD matrix, *in vivo* and its wound healing ability in type I and type II diabetic mice. The findings of this study could highlight the potential use of the Dual-HCD matrix in wound healing.

## Materials and methods

### Synthesis of stabilized growth factors loaded hyaluronate collagen dressing

The hyaluronate collagen dressing (HCD) matrix was synthesized as previously described.<sup>28</sup> Briefly, collagen, hyaluronic acid, and pluronic F68 were dissolved in refined water and adjusted pH to 7–8. Then, the different concentration ratios of structurally stabilized EGF (S-EGF) and bFGF (S-bFGF) were added and mixed with HCD matrix solution (Table S1). Aliquoted mixture into the mold for liphophilization.

### Cell viability test

The Balb/3T3 and NIH/3T3 fibroblast cells were cultured in Dulbecco's modified Eagle medium high-glucose (DMEM-HG; Gibco, Carlsbad, CA, USA) supplemented with 10% fetal bovine serum (FBS, Gibco) and 1% antimycotic solution (Gibco) in a 5% CO<sub>2</sub> humidified atmosphere at 37°C.<sup>40,41</sup> Each cells were seeded at a density of  $3 \times 10^3$  cells/well on 96 well plates and incubated for 24 h. The HCD matrix containing different concentration ratios of the S-EGF and S-bFGF were added in medium of each well and the cells were subsequently starved in serum-free DMEM medium for 72 h. Then thiazolyl blue tetrazolium bromide (MTT, M2128-100MG; St. Louis, MO, USA Sigma-Aldrich) was added. After 1.5 h of incubation, the absorbance was read at 450 nm.<sup>42</sup>

### Generation of streptozotocin (STZ)-induced type I diabetic mouse model and efficacy test of HCD matrix on type I diabetes

ICR mice (Male, 6 weeks old) were received from Orient Bio (Seoul, Korea). Streptozotocin (STZ, 200 mg/kg body weight; Sigma-Aldrich) was administered intraperitoneally to induce type I diabetes. STZ was dissolved in 0.05 M citrate buffer (pH 4.5).<sup>43,44</sup> Seven days post-injection, the blood glucose levels were measured after 12 h of fasting using the OneTouch Select meter (Johnson & Johnson, New Brunswick, NJ, USA). Approximately 5  $\mu$ L of mouse blood obtained from the caudal vein was used to measure the blood glucose level. In our previous study, the blood glucose level was maintained above 300 mg/dL for 3 weeks in diabetic mice.<sup>45</sup> Thus, we decided that blood glucose level should be higher than 300 mg/dL to be confirmed as a type I diabetic mouse model. To evaluate the

efficacy of the HCD matrix, we categorized the mice into five groups. The groups were as follows: DEFECT (untreated negative control group), HCD only (a group treated with HCD), and HCDEF (a group treated with S-EGF:S-bFGF (2:1 ratio) at a total concentration of  $1 \mu\text{g}/\text{cm}^2$ , S-EGF:S-bFGF (1:1 ratio) at a total concentration of  $1 \mu\text{g}/\text{cm}^2$ , S-EGF:S-bFGF (1:2 ratio) at a total concentration of  $1 \mu\text{g}/\text{cm}^2$ ). The matrix was replaced every 2 days. Reduced wound closure sites were confirmed at days 0, 3, 7, 10, and 14. The animal experiments were carried out in accordance with the guidelines set by the Department of Laboratory Animal Resources (Permit No. 2017-0016).

### **Development of type I and type II diabetic mouse model with defective wound healing**

The type II diabetic mice (C57BL/ksJ db/db, Male, 8 weeks old) were purchased from Central Lab Animal Inc. (Korea). The process for developing a mouse model with defective wound healing associated with diabetes has been outlined in our previous study.<sup>45</sup> Briefly, mice were anesthetized via administration of Zoletile (30 mg/kg body weight) and Rumpun, (10 mg/kg body weight), intraperitoneally. The hair on the back of the mouse was shaved, and the skin was sterilized using 70% ethanol. Full-thickness skin wounds of a diameter of 10 mm were made on the backs of STZ-induced type I and II diabetic mice. Wound contraction was prevented by fixing it with a silicone ring around the wound site. After application of the matrix on the wound site, vaseline gauze (Covidien, St. Louis, MO, USA) and neo dressing (Everaid, Gangnam, Seoul, Korea) were placed on the matrix to minimize the dehydration of wound sites. Type I diabetic mice were then sacrificed at 14 days post-operation ( $n=5$  per each group). While type II diabetic mice were sacrificed at 14 and 21 days post-operation ( $n=40$  and  $n=20$  per time point).

### **Biocompatibility test**

For biological safety test of Dual-HCD matrix, the Dual-HCD matrix was applied on full-thickness skin wounds of Sprague-Dawley rats (male, 8 weeks old,  $n=5$  in each group). Groups were classified into control (HCD matrix) and Dual-HCD matrix groups. After implantation, the rats were sacrificed, and skin tissue was harvested at days 7 and 14. The skin tissues were fixed in 3.7% formaldehyde before hematoxylin and eosin (H&E) staining.

### **Measurement of wound closure**

The images of the wounds were captured on days 0, 3, 7, 10, and 14 for type I diabetic mice and on days 0, 3, 7, 10, 14, 17, and 21 for type II diabetic mouse using a digital camera (Nikon, Tokyo, Japan). The degree of wound closure was evaluated by measuring the initial and remaining

wound area using Image J v.1.8.0 software (Aspire Software International, Leesburg, VA, USA). The formula used to calculate the remaining wound area was as follows:

$$\text{Relative wound area (\%)} = \frac{(A_o - A_t)}{A_o} \times 100$$

where  $A_o$  is the initial wound area on day zero and  $A_t$  is the regenerated wound area on the indicated date. The completion of wound repair was defined as a wound area equal to the area on day zero.

### **Histological analysis of regenerated tissues**

Type I and II diabetic mice were sacrificed on days 14 and 21 post-implantation respectively. And then, 5 wound tissues per each group were used for histological analysis. The tissues were fixed in 3.7% formaldehyde. Re-epithelialization and neovascularization were comparatively analyzed using H&E staining, while collagen deposition was analyzed using Masson's trichrome (MT) staining. They were quantitatively measured using Image J software. We followed the protocol used in a previous study for the quantitative measurement of the wounds.<sup>45</sup>

### **Immunofluorescence**

Resected skin tissue samples from the wound area were fixed in 3.7% formaldehyde. The skin tissue was embedded in paraffin, deparaffinized, rehydrated, and washed with phosphate buffer saline (PBS; Gibco). To confirm neovascularization, anti-CD31 (50:1; Abcam, Cambridge, MA, USA) was used as the primary antibody. Phycoerythrin (PE)-conjugated goat anti-rabbit secondary antibodies (Santa Cruz Biotechnology INC., CA, USA) were used to visualize the primary antibody. To observe fibroblasts,  $\alpha$ -smooth muscle actin ( $\alpha$ -SMA) (200:1, Santa Cruz) was used as the primary antibody, and fluorescein isothiocyanate (FITC)-conjugated goat anti-mouse secondary antibodies (Santa Cruz) were used. Nuclei were stained with DAPI (4',6-diamidino-2-phenylindole, Sigma-Aldrich). Images were acquired using a fluorescence microscope (IX-71; Olympus, Tokyo, Japan).

### **HMGB1 secretion level**

Human keratinocyte (HaCaT) cell line was kindly gifted from Dr. Min-Geol Lee (Yonsei University College of Medicine, Seoul, Korea).<sup>46</sup> The HaCaT cells were seeded onto the lower chamber, and the different types of HCD matrix were placed in the upper chamber of the transwell 6 well plate. After 48 h, the supernatant was collected from the HaCaT cells seeded onto the lower chamber. The

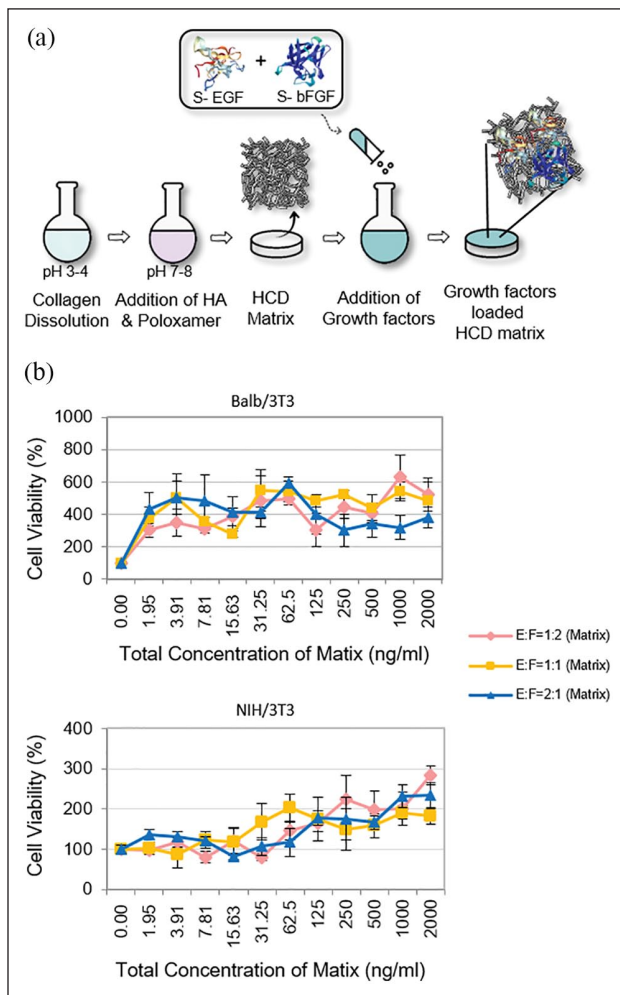


**Figure 1.** Different concentration ratios of S-EGF and S-bFGF loaded HCD matrices were synthesized and evaluated in vitro. (a) Schematic illustration of S-EGF and S-bFGF loaded HCD matrix production. (b) The cytotoxicity of stabilized EGF and bFGF loaded HCD matrix was analyzed in Balb/3T3 and NIH/3T3 fibroblast cell. The S-EGF:S-bFGF (1:1, 1:2, 2:1) HCD matrix with various concentrations were used.

supernatant was then concentrated using Amicon® Ultra Centrifugal Filters (Millipore, MA, USA). Further, the filtered supernatant was centrifuged for 1 h at 4°C, and then the samples were boiled at 100°C for 5 min to perform western blotting. Total protein was extracted from HaCaT cells. The cells were lysed using a PRO-PREP protein extraction solution (Intron, Sung-nam, Korea). The protein concentrations were determined using the BCA assay kit (Intron). Equal amounts of proteins (25°C µg) were subjected to 10% sodium dodecyl sulfate-polyacrylamide gel electrophoresis (SDS-PAGE) and then transferred onto polyvinylidene difluoride (PVDF) membranes (Hybond Escondido, CA, USA). The membranes were blocked using 5% skimmed milk (BD Biosciences, CA, USA) for 1 h at room temperature (20–25°C). Immunoblots were probed with the indicated antibodies against HMGB1 (Abcam,

Cambridge, UK) and β-actin (Santa Cruz, Texas, USA) at 4°C overnight.

### In vitro scratch wound closure assay

A scratch assay was performed using the HaCaT cells to measure cell migration in vitro. HaCaT cells were maintained in DMEM-HG (Gibco) supplemented with 10% FBS (Gibco) and 1% antibiotic antimycotic solution (Gibco) at 37°C with 5% CO<sub>2</sub>. The cells were then seeded onto a 6-well plate at a density of  $1.5 \times 10^5$  cells/well and cultured as a monolayer to achieve confluence overnight. When the cells reached 100% confluence, the scratch wounds were introduced using a sterile 20–200 µL pipette tip. Following scratch formation, HaCaT cells were treated with the recombinant protein S-EGF (0.3 µg) and S-EGF+S-bFGF (1:2, 1 µg of total protein). The cells were then incubated in DMEM-HG (Gibco) supplemented with 1% FBS (Gibco) in a 5% CO<sub>2</sub> humidified atmosphere at 37°C. The scratch closure was quantified by measuring the scratch area at 0 and 48 h post wounding. The images were captured using a microscope (TS100, Nikon, Japan).

### Statistical analysis

Student's *t*-test and ANOVA were performed for statistical analysis. Data are expressed as the mean ± standard deviation (SD). For all tests, \**p* < 0.05, \*\**p* < 0.01, \*\*\**p* < 0.001 were considered statistically significant.

## Results

### Characterization of stabilized growth factors loaded HCD matrix

The hyaluronate collagen dressing (HCD) matrix loaded with different concentration ratios of stabilized growth factors was developed and schematic illustration showed brief process of producing stabilized growth factors loaded HCD matrix (Figure 1(a)). We evaluated cell viability of S-EGF and S-bFGF loaded HCD matrix in Balb/3T3 and NIH/3T3 fibroblast cell. As a result, the percentage cell viability of the stabilized growth factors loaded HCD matrices (S-EGF:S-bFGF at the ratios of 1:1, 1:2, 2:1) exhibited no significant differences between the groups. Especially, the HCD matrix loaded with S-EGF and S-bFGF in the ratio of 1:2 efficiently enhanced the activity of cell proliferation (Figure 1(b)).

### Determination of the optimal concentration ratio of S-EGF and S-bFGF in an STZ-induced type I diabetic mouse model

In our previous study, we confirmed that the stabilized growth factors alone—stabilized-EGF (S-EGF) and bFGF



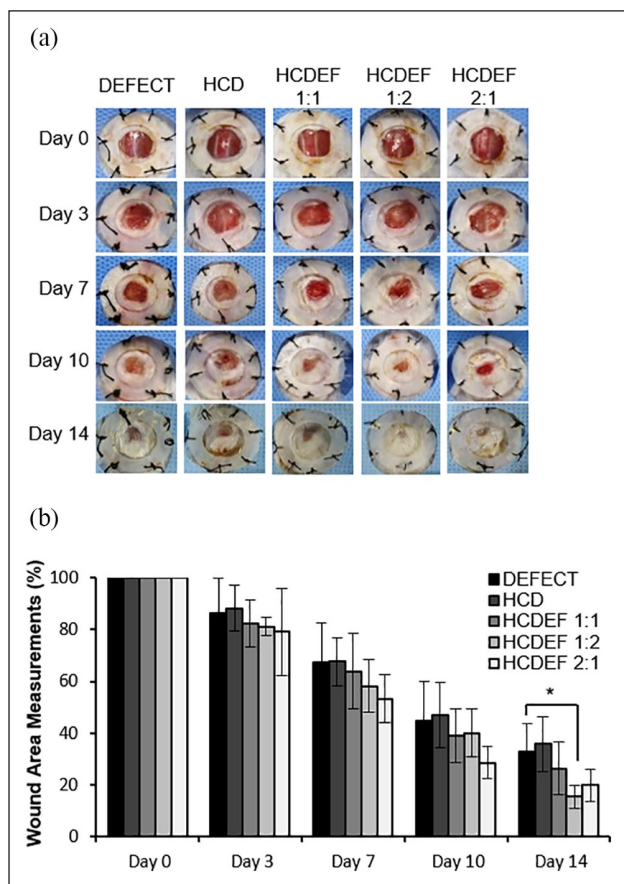


**Figure 2.** Optimal concentration ratio of S-EGF and S-bFGF was determined in the STZ-induced mouse model of type I diabetes. HCDEF (S-EGF:S-bFGF (1:1) at a total concentration of  $1 \mu\text{g}/\text{cm}^2$ , S-EGF:S-bFGF (1:2) at a total concentration of  $1 \mu\text{g}/\text{cm}^2$ , and S-EGF:S-bFGF (2:1) at a total concentration of  $1 \mu\text{g}/\text{cm}^2$ ) was applied to full-thickness skin wounds in type I diabetic mice. (a) Images were captured on days 0, 3, 7, 10, and 14. (b) Quantitative analysis of the wound area was measured. \* $p < 0.05$  versus DEFECT.

(S-bFGF)—with hyaluronate collagen dressing (HCD) matrix promote wound healing in a diabetic mouse model.<sup>29</sup> In this study, an STZ-induced mouse model of type I diabetes was used to establish the optimal concentration ratio of S-EGF and S-bFGF that can induce effective wound healing. Cytotoxicity assay was performed using elutes of the double growth factor-loaded matrix. None of the treatment groups, S-EGF with HCD (HCDE), S-FGF with HCD (HCDF), and S-EGF/S-FGF with HCD (HCDEF), showed significant cytotoxicity when compared to the negative control group. These results indicated that growth factor-loaded materials were not cytotoxic (data not shown). We observed that the HCDEF groups showed greater wound healing capacity than HCD and DEFECT groups 10 days after implantation (Figure 2(a) and (b)). Particularly, among the three different concentration ratios used, the mice treated with S-EGF:S-bFGF in the ratio 1:2, referred to as Dual-HCD in this study, showed greater wound healing capacity on day 14 than the other

groups. In accordance with this result, the re-epithelialization and collagen deposition rates were also found to be increased in the Dual-HCD group (as shown in Figures S1 and S2). The cumulative amount of released S-EGF and S-bFGF from the Dual-HCD matrix was confirmed to be over 97% within 3 days (Figure S3). As part of the biological safety test, we applied the Dual-HCD matrix on full-thickness skin wounds on a Sprague-Dawley rat. We observed that the Dual-HCD matrix had no inflammation reaction (Figure S4). Therefore, we confirmed the optimal concentration ratio of S-EGF:S-bFGF to be 1:2.

### Wound healing effect of Dual-HCD matrix in type II diabetic mice

To evaluate the wound healing capacity of Dual-HCD on diabetic wounds, we used a type II diabetic mouse model. Type I diabetes is issued due to insulin deficiency by the destruction of pancreatic beta cells, while Type II diabetes is caused by dysfunction of insulin. Around 90% of diabetic patients have type II diabetes.<sup>47,48</sup> The Dual-HCD matrix was applied to full-thickness skin wounds on type II diabetic mice. The HCDE (HCD loaded with EGF only) group was used as a comparative group to evaluate a single growth factor effect.<sup>29</sup> The Dual-HCD group showed greater wound healing capacity after day 14, compared to DEFECT, HCD, and HCDE groups. Specifically, the wound closure rate of HCDE and Dual-HCD groups had increased by 1.4- and 2.4- fold, respectively, compared to that of the DEFECT group (Figure 3(a)). The HCDE group showed a higher wound closure rate at day 14 than the DEFECT and HCD only groups. However, it was less effective than the Dual-HCD group. The wound closure in the Dual-HCD group was significantly promoted from day 14 after implantation, and it had completely closed by day 21, while more than 10% of the wound remained in all the other groups (Figure 3(b)).

### Wound re-epithelialization ability by Dual-HCD matrix in type II diabetic mice

Next, we carried out Masson's trichrome (MT) staining on day 21 to further evaluate epithelial layer regeneration at the wound site. The Dual-HCD group showed excellent tissue regeneration capacities compared to that of DEFECT and HCDE groups. The tissue of the Dual-HCD group had completely regenerated on day 21 (Figure 4(a)). To be specific, the Dual-HCD group demonstrated about 2.7-fold higher capacity of re-epithelialization compared to the DEFECT group (Figure 4(b)).

### Neovascularization ability of Dual-HCD in regenerated tissues of type II diabetic mice

To further investigate the neovascularization ability of Dual-HCD matrix, hematoxylin and eosin (H&E) staining

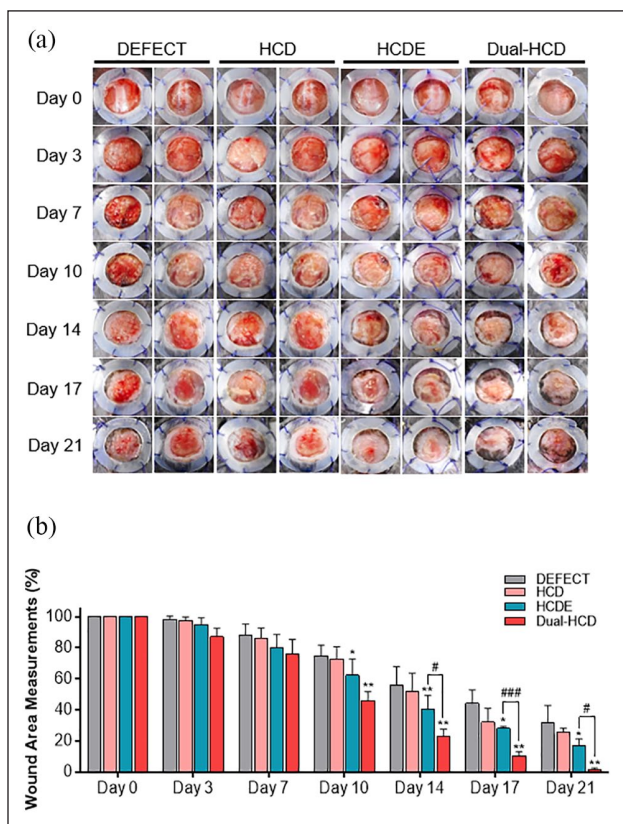


**Figure 3.** Dual-HCD significantly enhanced wound healing capacity in type II diabetic mice. HCDE (at a total concentration of  $0.3 \mu\text{g}/\text{cm}^2$ ) and Dual-HCD (S-EGF:S-bFGF (1:2) at a total concentration of  $1 \mu\text{g}/\text{cm}^2$ ) were applied to full-thickness skin wounds in type II diabetic mice. (a) Images of the wound sites were captured on days 0, 3, 7, 10, 14, 17, and 21. (b) The wound closure rate was quantitatively analyzed.

\* $p < 0.05$ . \*\* $p < 0.01$  versus DEFECT.

# $p < 0.05$ . ### $p < 0.001$  versus HCDE.

and immunohistochemistry for CD31 and alpha-smooth muscle actin ( $\alpha$ -SMA) labeling were performed on day 14. The result indicated that Dual-HCD formed extensive red capillary vasculature compared to the other treatments. In accordance with the results of H&E staining (Figure 5(a)), immunofluorescence showed that a higher number of CD31-expressing cells was detected in the Dual-HCD group than in the other groups (Figure 5(b)). Especially, the quantitative analysis of CD31-positive cells revealed that the number of CD31-positive cells in the Dual-HCD group was 23.6- and 2.4-fold higher than that in the DEFECT and HCD groups, respectively (Figure 5(d)). Moreover, the expression of  $\alpha$ -SMA, the biomarker of mural cells in blood vessels, was detected via immunofluorescence labeling. The results demonstrated that the number of  $\alpha$ -SMA expressing cells was significantly higher in the Dual-HCD group than in DEFECT, HCD, and HCDE groups (Figure 5(c)). Quantitative analysis revealed that the number of  $\alpha$ -SMA expressing cells was 11-fold higher

in the Dual-HCD matrix-applied group and 6.4-fold higher in the HCDE matrix applied group, as compared to that in the DEFECT and HCD groups (Figure 5(e)). We also observed that the Dual-HCD group achieved a faster revascularization rate as compared to that of the other groups.

### Collagen deposition in type II diabetic mice

The deposition rates and alignment of collagen were evaluated via MT staining in the regenerated tissue area. The MT staining was performed on day 21 after implantation. MT staining revealed greater deposition of collagen at the wound site of HCDE and Dual-HCD groups than that of the DEFECT group. Notably, the Dual-HCD group displayed greater alignment and deposition of collagen in the newly formed tissues than the HCDE group (Figure 6(a)). Collagen deposition rates in the wound sites were also quantitatively analyzed. The rate of collagen deposition in the Dual-HCD group was 6.3- and 4.9-fold higher than that in the DEFECT and HCD groups, respectively (Figure 6(b)).

### Chemotactic effects of double growth factors

To investigate the secreted HMGB1 protein levels from the HaCaT cells induced by double growth factors, western blotting was performed using supernatant obtained from the growth factor-loaded matrix. We observed that a considerable increase in HMGB1 secretion level was detected where the Dual-HCD matrix was applied (Figure 7(a) and (b)). The results of in vitro scratch assay demonstrated a significant difference between scratch wound closure at 0 h and 48 h in the presence of growth factors. As expected, the HaCaT cells of groups treated with double growth factors showed significantly higher wound closure rate than groups not treated with growth factors and those treated with a single growth factor (Figure 7(c) and (d)). This implies that enhanced chemotactic migration was induced by the synergistic effect of a combination of S-EGF and S-bFGF.

## Discussion

Each phase of wound healing requires multiple factors such as pro-inflammatory cytokines and growth factors including transforming growth factor (TGF)- $\beta$ , vascular endothelial growth factor (VEGF), FGF, and EGF.<sup>18,49,50</sup> All phases must occur at a specific time with optimal interactions between signals and molecules for a wound to heal completely. However, the dysregulation of several cellular functions in diabetic wounds, such as impaired migration of keratinocytes and fibroblasts, extracellular matrix (ECM) deposition, defects in T-cell immunity, and upregulation of metalloproteases, results in chronic and impaired

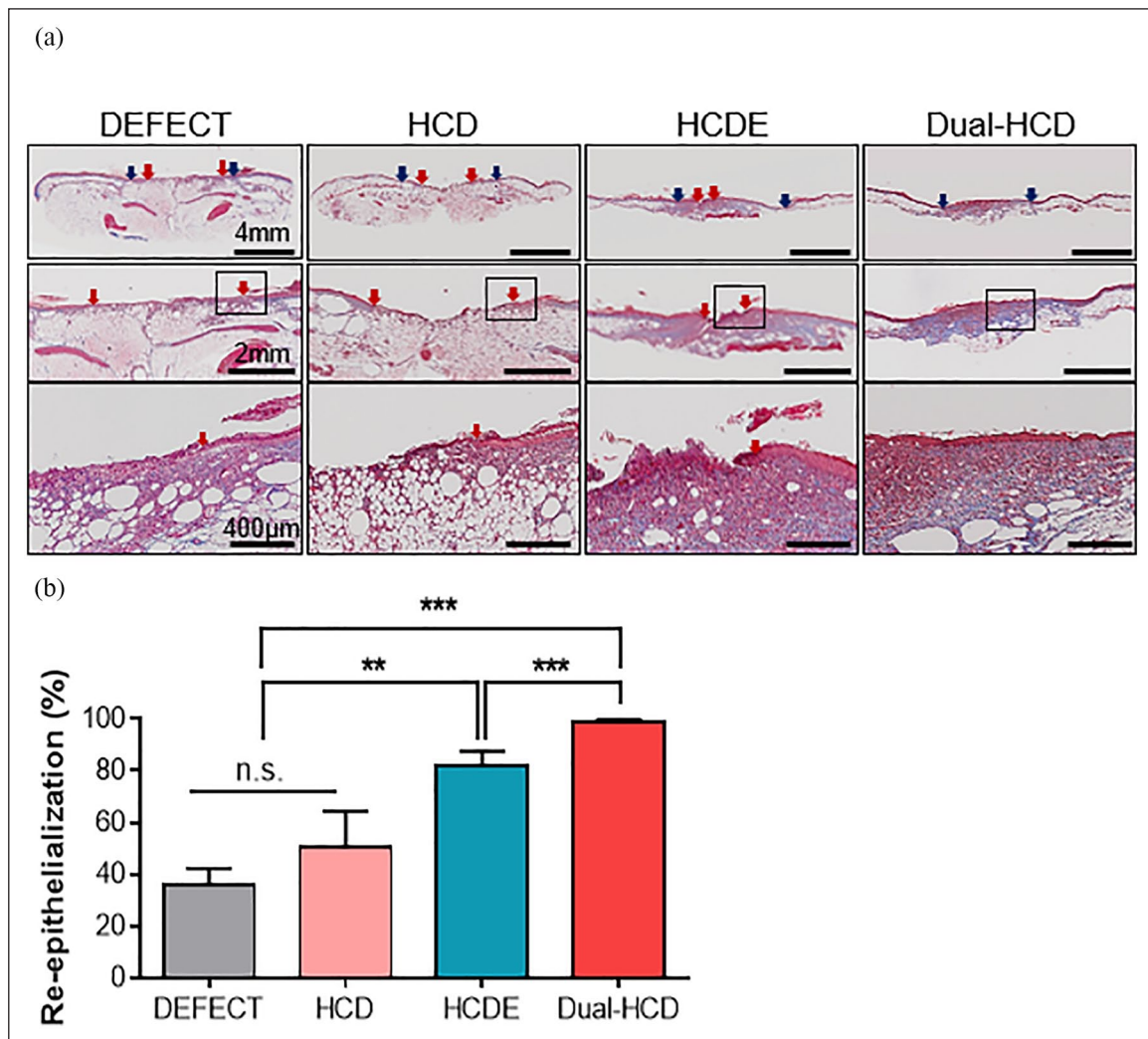


**Figure 4.** Dual-HCD matrix significantly promoted the regeneration of epithelial layer at the wound sites. (a) Images present re-epithelialization of the damaged skin tissues in the DEFECT, HCD, HCDE, and Dual-HCD groups. Blue arrows indicate the edge of the wounds, while red arrows indicate the wound epithelial margins. The distance between the two red arrows marks the width of the unrecovered epithelial layer. Scale bars = 4 mm, 2 mm, 400  $\mu$ m. (b) The regenerated epithelial layer was quantitatively analyzed. n.s.; >0.5.

\*\* $p < 0.01$ . \*\*\* $p < 0.001$  versus DEFECT.

wounds.<sup>51</sup> Moreover, the growth factors are also dysregulated in individuals with diabetes mellitus. Although wound healing is an automatic process involved in the recovery of injured skin tissue, wound repair and regeneration are delayed under diabetic conditions, resulting in impaired wound healing.<sup>7,38,39</sup> EGF is known to enhance re-epithelialization by promoting migration and proliferation of keratinocytes, while bFGF helps to stimulate neovascularization to trigger wound healing.<sup>23–26</sup> Since EGF and bFGF play a major role in the wound healing process, several studies have been conducted for their clinical application and numerous wound-dressing materials containing growth factors have been developed. Despite its therapeutic effects, the use of EGF and bFGF in wound healing is limited due to their short half-life and

low stability at room temperature.<sup>27,52,53</sup> This leads to the inactivation of growth factors when they are loaded onto a matrix. Wound dressing materials could be used as a protective barrier against pathogens. However, wound dressing materials are generally unstable and are difficult to be applied directly onto the skin as they usually melt right after contact with body fluids.<sup>54</sup> Thus, it is not suitable to protect the wounds and effectively deliver growth factors into the wounds. Therefore, we developed S-EGF and S-bFGF in our previous study to overcome the limitations of the use of growth factors. Their biological stability was confirmed as well. Furthermore, we also developed an HCD matrix to deliver growth factors efficiently into the wounds.<sup>28</sup> The HCD matrix has several advantages such as hemostatic effect, reduction of pain, and maintenance of



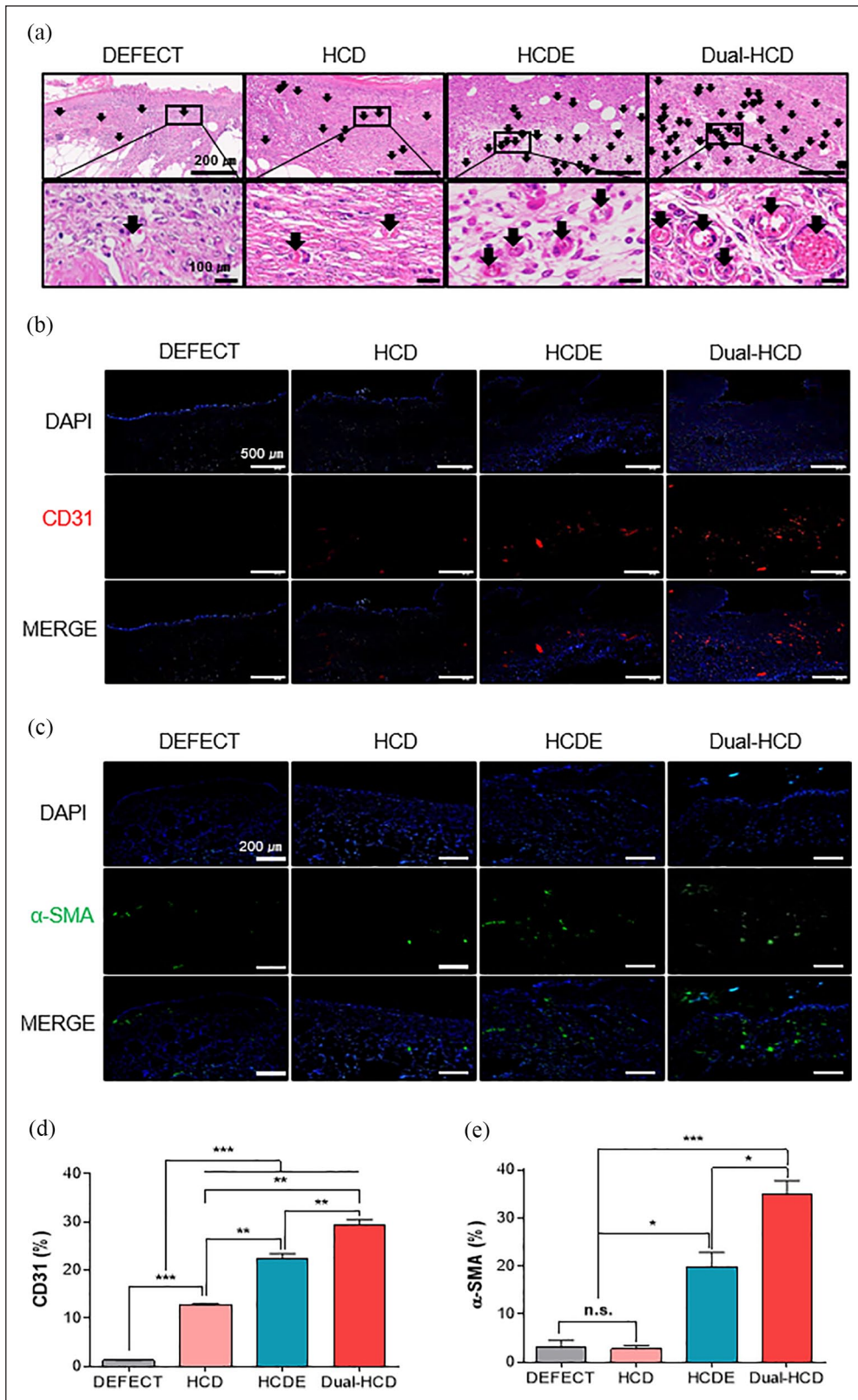


**Figure 5.** Effect of Dual-HCD on neovascularization at the wound site. (a) H&E staining was performed on day 14 post-operation. Arrows in the image indicate capillary vasculatures. Scale bars = 200 μm, 100 μm. (b) Immunohistochemistry was performed to label CD31-positive cells (red) on day 14. Scale bars = 500 μm. (c) Immunofluorescence images indicating the presence of α-SMA expression mural cells (green) with DAPI (blue) nuclear staining on day 21 after implantation. Scale bars = 200 μm. (d, e) CD31-expressing cells and α-SMA-positive cells were quantitatively analyzed using Image J software. \**p* < 0.05. \*\**p* < 0.01. \*\*\**p* < 0.001.



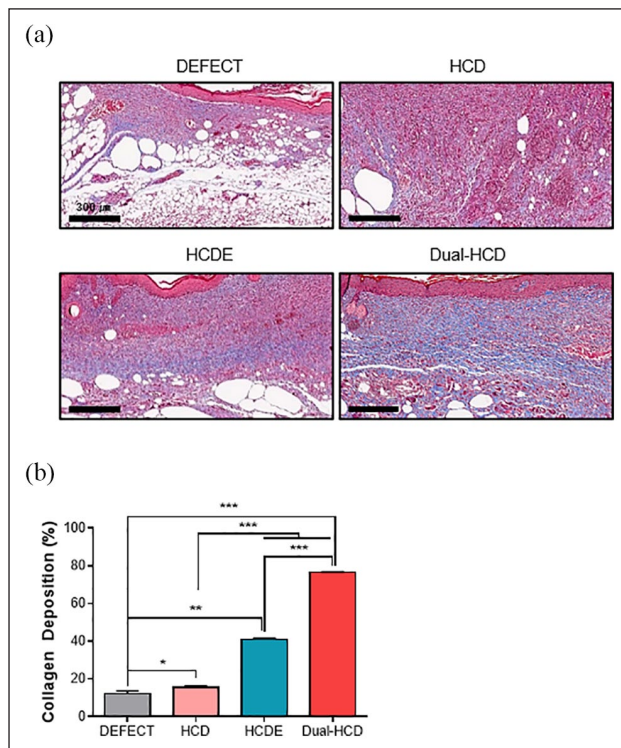


**Figure 6.** Dual-HCD matrix improved collagen deposition in regenerated tissue. (a) MT staining was performed to observe collagen alignment on day 21 post-implantation. Blue areas in the image present the newly formed collagen tissue. Scale bars = 300  $\mu$ m. (b) To quantify collagen deposition in the wound area, images were analyzed using Image J software. \* $p < 0.05$ . \*\* $p < 0.01$ . \*\*\* $p < 0.001$ .

moisturizing environment around the wound area. Additionally, the HCD matrix does not adhere to the wound. These advantages make the HCD matrix suitable to be used as a base material for wound dressing.<sup>28,29</sup> We also confirmed the positive effect of stabilized growth factor alone, either S-EGF or S-bFGF, with HCD matrix in diabetic mouse model which showed great improvement in wound healing.<sup>29</sup>

Based on our previous study, we speculated that the combination of S-EGF and S-bFGF would generate a synergistic effect in impaired wound healing. Prior to the animal, we checked the cytotoxicity of the HCD matrix that was loaded with multiple combinations of growth factors. Dual-HCD in the ratio of 1:2 (S-EGF:S-bFGF) was confirmed to be effective. Thus, we developed a Dual-HCD matrix. It showed greater enhancement of wound healing capacity as compared to a single growth factor-loaded HCD matrix. These data indicate that the optimal ratio of the concentration of growth factors is 1:2 and that they are biologically safe to be used as a wound dressing material, especially in case of impaired wound healing.

Based on the above results, in this study, we aimed to assess the wound healing capacity of the Dual-HCD matrix

in type II diabetic mice. Since we have already confirmed its effect in type I diabetic mice, we attempted to demonstrate it in type II diabetic mice. The type II diabetes mellitus mouse model exhibits severe impairments in wound healing as compared to the type I diabetes mellitus mouse model.<sup>55</sup> Moreover, type II diabetic mice are appropriate mouse models that mimic the pathophysiological features observed in humans.<sup>56</sup> To evaluate the effect of the growth factor-loaded matrix on the wound closure rate during the healing process, either S-EGF alone or Dual-HCD matrix was applied to the wound sites in type II diabetic mice. As a result, we observed that the S-EGF alone with HCD matrix promoted wound healing, but the Dual-HCD group achieved faster closure of the diabetic skin wounds; wounds were completely closed on day 21 post-implantation. The tissue regeneration rates around the wound site showed greater enhancement in the Dual-HCD group than in DEFECT, HCD, and HCDE groups. Specifically, the Dual-HCD group induced perfectly closed wound site, while DEFECT, HCD, and HCDE groups showed 74%, 50%, and 18% of uncovered wound sites, respectively.

Angiogenesis in the dermis is crucial for effective wound healing. Angiogenesis comprises multiple steps that require migration and proliferation of epithelial and mural cells to form blood vessels and deliver sufficient amounts of oxygen, various nutrients, and growth factors that are necessary for wound healing.<sup>57,58</sup> Nonetheless, studies have reported that abnormalities of angiogenesis are observed in diabetes mellitus.<sup>59</sup> For evaluation of neovascularization of the wounds, we performed H&E staining and immunohistochemistry to verify whether the enhanced wound healing capacity in diabetic mice with Dual-HCD matrix was due to increased angiogenesis. The results of the H&E staining revealed that the Dual-HCD group showed a denser capillary vascular network than the other groups. Moreover, since CD31 and  $\alpha$ -SMA are the markers of endothelial and mural cells in blood vessels, we also quantified the expression of CD31 and  $\alpha$ -SMA in wound skin tissues using immunofluorescence. Immunofluorescence detection of CD31 and  $\alpha$ -SMA was performed on day 14 post-implantation. The expression of both markers was highly detected in mice belonging to the Dual-HCD group. Accordingly, quantitative analysis showed that the Dual-HCD group showed 23.6- and 2.36-fold greater number of CD31 expressing cells than the DEFECT and HCD groups, respectively. Quantitative analysis of  $\alpha$ -SMA-positive cells revealed that the Dual-HCD group exhibited 11.4- and 12.6-fold higher capacity for neovascularization, as compared to DEFECT and HCD groups, respectively. The DEFECT and HCD groups did not differ significantly.

The collagen in the ECM, is a crucial component in the terminal stage of wound healing. During the maturation stage of wound healing, collagen synthesis, deposition, and alignment increases as the tissues are regenerated. Collagen formation rarely occurs in the early stage of

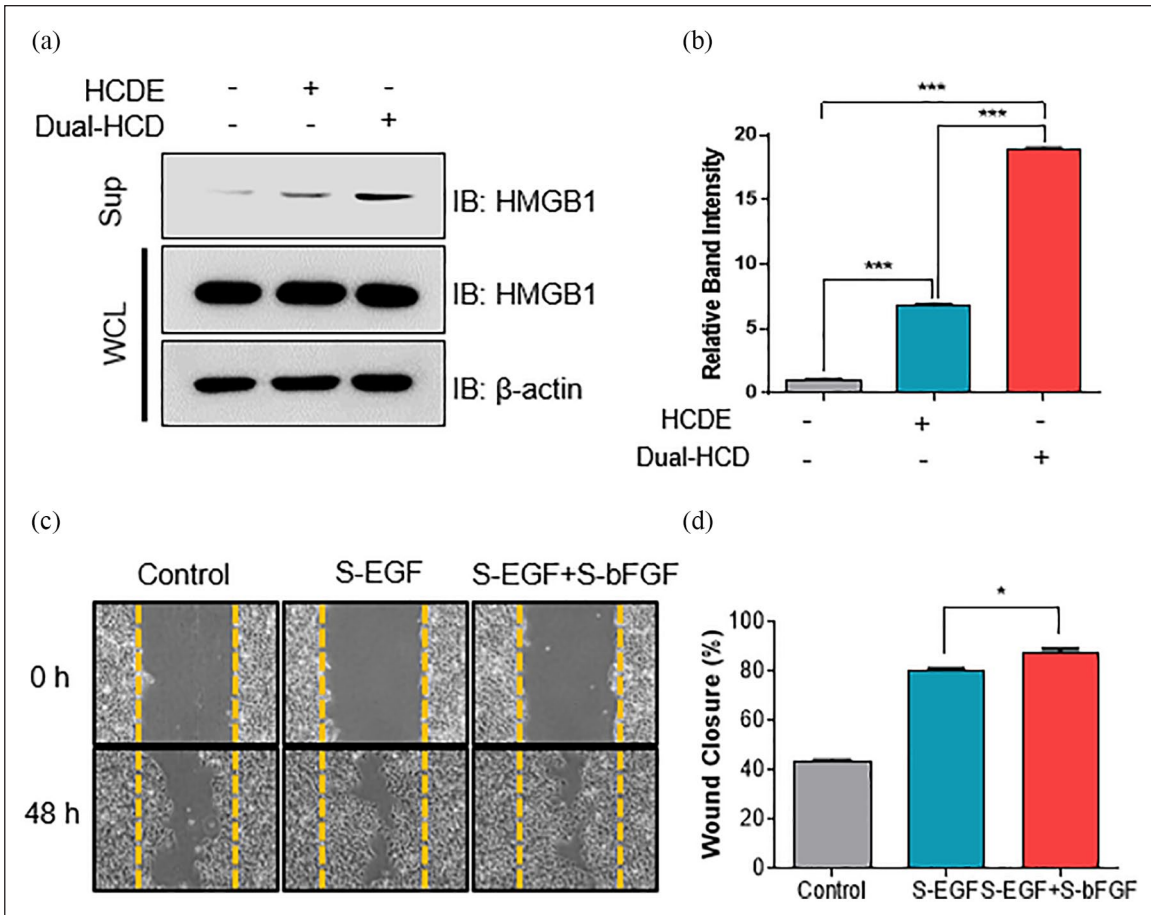


**Figure 7.** Double growth factors promoted the secretion of HMGB1 and increased the wound closure rate in HaCaT cells. (a) The supernatant was obtained from the HaCaT cells, where the HCD matrices were applied. The secreted HMGB1 protein level was detected using western blot analysis. (b) Relative band intensity was analyzed using Image J software. (c) The images demonstrating wound migration was captured at 0 and 48h after wound scratching. The concentrations of treated recombinant proteins were 0.3  $\mu$ g/mL (S-EGF) and 1  $\mu$ g/mL (1:2 ratio, S-EGF+S-bFGF). (d) The wound closure percentage was measured using Image J software. \* $p < 0.05$ . \*\*\* $p < 0.001$ .

wound healing. Thus, only minimal collagen deposition can be observed. MT staining of wound skin sections on day 21 further confirmed the deposition and alignment of newly synthesized collagen. The result demonstrated that the Dual-HCD group showed extensive staining, indicating that it had the highest collagen deposition. Moreover, their collagen fibers were orderly arranged. The DEFECT and HCD group exhibited significantly more disorganized collagen fibers in the dermis than HCDE and Dual-HCD groups. The HCDE group also showed ordered arrangement of collagen fibers, but its staining was less intense than that of the Dual-HCD group. Accordingly, Dual-HCD showed 76.5% of collagen deposition, whereas 12.1%, 15.6%, and 40.9% collagen deposition was observed in DEFECT, HCD, and HCDE groups, respectively.

The cytokine HMGB1 is known to induce chemotaxis, cell proliferation, and vessel formation, which results in improved cell migration, re-epithelialization, and neovascularization during the wound healing process.<sup>32,60,61</sup>

However, downregulation of HMGB1 in diabetic humans and mice have already been reported in previous studies.<sup>32</sup> The downregulation of HMGB1 delays the wound healing process. Several studies have already stressed the importance of HMGB1 in the wound healing process,<sup>32,34,62</sup> and it is already known that HMGB1 increases the level of growth factors.<sup>35,63,64</sup> However, a few studies have demonstrated the role of growth factors in promoting HMGB1. Thus, in this study, we aimed to confirm whether double growth factors enhance HMGB1 expression levels. We observed that the combined application of the growth factor-loaded HCD matrix promotes the secretion of HMGB1 in vitro. We also established a scratch wound healing model to investigate the effects of growth factors on wound healing and cell migration using monolayer culture. HaCaT cells are keratinocytes that mimic the properties of epidermal keratinocytes. Furthermore, HaCaT cells have a similar migration index as human primary keratinocytes, and the growth factors positively affect wound healing that

stimulates epithelial cells and thereby enhances wound closure.<sup>65</sup> Consequently, the HaCaT cells with double growth factors achieved a much faster wound closure rate than those of the other groups and thus exhibited narrower denuded regions of wounds than cells cultured in the absence of any growth factors and those treated only with S-EGF.

## Conclusions

In this study, we developed a Dual-HCD (S-EGF: S-bFGF, 1:2, 1  $\mu\text{g}/\text{cm}^2$ ) matrix, which possesses the ability to accelerate diabetic wound healing. Our results demonstrated that the application of the Dual-HCD matrix onto the wound area induced re-epithelialization, neovascularization, and collagen deposition. We also established that, in vitro, the migration of HaCaT cells was significantly stimulated to a greater extent when treated with the combination of S-EGF and S-bFGF than the cells treated with a single growth factor (S-EGF). Additionally, HMGB1 levels increased in cells treated with double growth factors, S-EGF, and S-bFGF. Altogether, we demonstrated that the Dual-HCD matrix exhibits a synergistic effect and thus provides insights into how Dual-HCD is better at enhancing wound healing than a single growth factor-loaded HCD. Based on these findings, we conclude that the Dual-HCD matrix could serve as an effective therapeutic agent for the treatment of chronic diabetic wounds.

## Declaration of conflicting interests

The author(s) declared no potential conflicts of interest with respect to the research, authorship, and/or publication of this article.

## Funding

The author(s) disclosed receipt of the following financial support for the research, authorship, and/or publication of this article: This work was supported by the Mid-career Researcher Program (NRF-2018R1A2B6007376) and by the Basic Science Research Program (NRF2020R111A1A01054892) through the National Research Foundation of Korea (NRF) funded by the Ministry of Education.

## ORCID iD

Kwang Hwan Park  <https://orcid.org/0000-0002-2110-0559>

## Supplemental material

Supplemental material for this article is available online.

## References

- King H and Rewers M. Global estimates for prevalence of diabetes mellitus and impaired glucose tolerance in adults. WHO Ad Hoc diabetes reporting group. *Diabetes Care* 1993; 16: 157–177.
- Shaw JE, Sicree RA and Zimmet PZ. Global estimates of the prevalence of diabetes for 2010 and 2030. *Diabetes Res Clin Pract* 2010; 87: 4–14.
- Ahmed I and Goldstein B. Diabetes mellitus. *Clin Dermatol* 2006; 24: 237–246.
- Daneman D. Type 1 diabetes. *Lancet (London, England)* 2006; 367: 847–858.
- DeFronzo RA, Ferrannini E, Groop L, et al. Type 2 diabetes mellitus. *Nat Rev Dis Primers* 2015; 1: 15019.
- Mehta SK, Breitbart EA, Berberian WS, et al. Bone and wound healing in the diabetic patient. *Foot Ankle Clin* 2010; 15: 411–437.
- Brem H and Tomic-Canic M. Cellular and molecular basis of wound healing in diabetes. *J Clin Invest* 2007; 117: 1219–1222.
- Zeng R, Lin C, Lin Z, et al. Approaches to cutaneous wound healing: basics and future directions. *Cell Tissue Res* 2018; 374: 217–232.
- Baltzis D, Eleftheriadou I and Veves A. Pathogenesis and treatment of impaired wound healing in diabetes mellitus: new insights. *Adv Ther* 2014; 31: 817–836.
- Barrientos S, Stojadinovic O, Golinko MS, et al. Growth factors and cytokines in wound healing. *Wound Repair Regen* 2008; 16: 585–601.
- Shen C, Sun L, Zhu N, et al. Kindlin-1 contributes to EGF-induced re-epithelialization in skin wound healing. *Int J Mol Med* 2017; 39: 949–959.
- Meyer M, Müller AK, Yang J, et al. FGF receptors 1 and 2 are key regulators of keratinocyte migration in vitro and in wounded skin. *J Cell Sci* 2012; 125: 5690–5701.
- Broadley KN, Aquino AM, Hicks B, et al. Growth factors bFGF and TGF beta accelerate the rate of wound repair in normal and in diabetic rats. *Int J Tissue React* 1988; 10: 345–353.
- Buckley A, Davidson JM, Kamerath CD, et al. Sustained release of epidermal growth factor accelerates wound repair. *Proc Natl Acad Sci USA* 1985; 82: 7340–7344.
- Grotendorst GR, Martin GR, Pencev D, et al. Stimulation of granulation tissue formation by platelet-derived growth factor in normal and diabetic rats. *J Clin Invest* 1985; 76: 2323–2329.
- Cross KJ and Mustoe TA. Growth factors in wound healing. *Surg Clin North Am* 2003; 83: 531–545.
- Bennett NT and Schultz GS. Growth factors and wound healing: Part II. Role in normal and chronic wound healing. *Am J Surg* 1993; 166: 74–81.
- Galkowska H, Wojewodzka U and Olszewski WL. Chemokines, cytokines, and growth factors in keratinocytes and dermal endothelial cells in the margin of chronic diabetic foot ulcers. *Wound Repair Regen* 2006; 14: 558–565.
- Goren I, Muller E, Pfeilschifter J, et al. Severely impaired insulin signaling in chronic wounds of diabetic ob/ob mice: a potential role of tumor necrosis factor-alpha. *American J Pathol* 2006; 168: 765–777.
- Falanga V. Wound healing and its impairment in the diabetic foot. *Lancet (London, England)* 2005; 366: 1736–1743.
- Barrientos S, Brem H, Stojadinovic O, et al. Clinical application of growth factors and cytokines in wound healing. *Wound Repair Regen* 2014; 22: 569–578.



22. Powers CJ, McLeskey SW and Wellstein A. Fibroblast growth factors, their receptors and signaling. *Endocr Relat Cancer* 2000; 7: 165–197.
23. Werner S and Grose R. Regulation of wound healing by growth factors and cytokines. *Physiol Rev* 2003; 83: 835–870.
24. Kwon YB, Kim HW, Roh DH, et al. Topical application of epidermal growth factor accelerates wound healing by myofibroblast proliferation and collagen synthesis in rat. *J Vet Sci* 2006; 7: 105–109.
25. Demirdogen B, Elcin AE and Elcin YM. Neovascularization by bFGF releasing hyaluronic acid-gelatin microspheres: in vitro and in vivo studies. *Growth Factors (Chur, Switzerland)* 2010; 28: 426–436.
26. Tonnesen MG, Feng X and Clark RA. Angiogenesis in wound healing. *J Investig Dermatol Symp Proc* 2000; 5: 40–46.
27. Dogan S, Demire S, Kepenekci I, et al. Epidermal growth factor-containing wound closure enhances wound healing in non-diabetic and diabetic rats. *Int Wound J* 2009; 6: 107–115.
28. Choi SM, Ryu HA, Lee KM, et al. Development of stabilized growth factor-loaded hyaluronate-collagen dressing (HCD) matrix for impaired wound healing. *Biomater Res* 2016; 20: 9.
29. Choi SM, Lee KM, Kim HJ, et al. Effects of structurally stabilized EGF and bFGF on wound healing in type I and type II diabetic mice. *Acta Biomater* 2018; 66: 325–334.
30. Sarkar SA, Lee CE, Victorino F, et al. Expression and regulation of chemokines in murine and human type 1 diabetes. *Diabetes* 2012; 61: 436–446.
31. Losi P, Briganti E, Errico C, et al. Fibrin-based scaffold incorporating VEGF- and bFGF-loaded nanoparticles stimulates wound healing in diabetic mice. *Acta Biomater* 2013; 9: 7814–7821.
32. Straino S, Di Carlo A, Mangoni A, et al. High-mobility group box 1 protein in human and murine skin: involvement in wound healing. *J Investig Dermat* 2008; 128: 1545–1553.
33. Zhang Q, O’Hearn S, Kavalukas SL, et al. Role of high mobility group box 1 (HMGB1) in wound healing. *J Surg Res* 2012; 176: 343–347.
34. Ranzato E, Patrone M, Pedrazzi M, et al. Hmgb1 promotes wound healing of 3T3 mouse fibroblasts via RAGE-dependent ERK1/2 activation. *Cell Biochem Biophys* 2010; 57: 9–17.
35. Biscetti F, Straface G, De Cristofaro R, et al. High-mobility group box-1 protein promotes angiogenesis after peripheral ischemia in diabetic mice through a VEGF-dependent mechanism. *Diabetes* 2010; 59: 1496–1505.
36. Ridiandries A, Tan JTM and Bursill CA. The role of chemokines in wound healing. *Int J Mol Sci* 2018; 19: 3217.
37. Chavakis E, Hain A, Vinci M, et al. High-mobility group box 1 activates integrin-dependent homing of endothelial progenitor cells. *Circ Res* 2007; 100: 204–212.
38. Rosenberg CS. Wound healing in the patient with diabetes mellitus. *Nurs Clin North Am* 1990; 25: 247–261.
39. Lan CC, Wu CS, Huang SM, et al. High-glucose environment enhanced oxidative stress and increased interleukin-8 secretion from keratinocytes: new insights into impaired diabetic wound healing. *Diabetes* 2013; 62: 2530–2538.
40. Śmieszek A, Czyrek A, Basinska K, et al. Effect of metformin on viability, morphology, and ultrastructure of mouse bone marrow-derived multipotent mesenchymal stromal cells and balb/3T3 embryonic fibroblast cell line. *Biomed Res Int* 2015; 2015: 769402.
41. Fazio E, Speciale A, Spadaro S, et al. Evaluation of biological response induced by molybdenum oxide nanocolloids on in vitro cultured NIH/3T3 fibroblast cells by micro-Raman spectroscopy. *Colloids Surf B Biointerfaces* 2018; 170: 233–241.
42. Mosmann T. Rapid colorimetric assay for cellular growth and survival: application to proliferation and cytotoxicity assays. *J Immunol Methods* 1983; 65: 55–63.
43. de la Garza-Rodea AS, Knaän-Shanzer S, den Hartigh JD, et al. Anomer-equilibrated streptozotocin solution for the induction of experimental diabetes in mice (*Mus musculus*). *J Am Assoc Lab Anim Sci* 2010; 49: 40–44.
44. Motyl K and McCabe LR. Streptozotocin, type I diabetes severity and bone. *Biol Proced Online* 2009; 11: 296–315.
45. Yoon DS, Lee Y, Ryu HA, et al. Cell recruiting chemokine-loaded sprayable gelatin hydrogel dressings for diabetic wound healing. *Acta Biomater* 2016; 38: 59–68.
46. Kim TG, Byamba D, Wu WH, et al. Statins inhibit chemotactic interaction between CCL20 and CCR6 in vitro: possible relevance to psoriasis treatment. *Exp Dermatol* 2011; 20: 855–857.
47. Goyal R and Jialal I. *Diabetes mellitus type 2. StatPearls*. Treasure Island, FL: StatPearls Publishing LLC, 2020.
48. Henderson S, Ibe I, Cahill S, et al. Bone quality and fracture-healing in type-1 and type-2 diabetes mellitus. *J Bone Joint Surg Am* 2019; 101: 1399–1410.
49. Schultz GS, Davidson JM, Kirsner RS, et al. Dynamic reciprocity in the wound microenvironment. *Wound Repair Regen* 2011; 19: 134–148.
50. Noh KC, Liu XN, Zhuan Z, et al. Leukocyte-poor platelet-rich plasma-derived growth factors enhance human fibroblast proliferation in vitro. *Clin Orthop Surg* 2018; 10: 240–247.
51. Guo S and Dipietro LA. Factors affecting wound healing. *J Dent Res* 2010; 89: 219–229.
52. Simons M, Annex BH, Laham RJ, et al. Pharmacological treatment of coronary artery disease with recombinant fibroblast growth factor-2: double-blind, randomized, controlled clinical trial. *Circulation* 2002; 105: 788–793.
53. Krishnamurthy R and Manning MC. The stability factor: importance in formulation development. *Curr Pharm Biotechnol* 2002; 3: 361–371.
54. Jacob S, Shirwaikar AA, Srinivasan KK, et al. Stability of proteins in aqueous solution and solid state. *Indian J Pharm Sci* 2006; 68(2): 154–163.
55. Michaels J, Churgin SS, Blechman KM, et al. Db/db mice exhibit severe wound-healing impairments compared with other murine diabetic strains in a silicone-splinted excisional wound model. *Wound Repair Regen* 2007; 15: 665–670.
56. Cefalu WT. Animal models of type 2 diabetes: clinical presentation and pathophysiological relevance to the human condition. *ILAR J* 2006; 47: 186–198.

57. Jain RK. Molecular regulation of vessel maturation. *Nat Med* 2003; 9: 685–693.
58. DeLisser HM, Christofidou-Solomidou M, Strieter RM, et al. Involvement of endothelial PECAM-1/CD31 in angiogenesis. *Am J Pathol* 1997; 151: 671–677.
59. Martin A, Komada MR and Sane DC. Abnormal angiogenesis in diabetes mellitus. *Med Res Rev* 2003; 23: 117–145.
60. Yang S, Xu L, Yang T, et al. High-mobility group box-1 and its role in angiogenesis. *J Leukocyte Biol* 2014; 95: 563–574.
61. Schiraldi M, Raucci A, Muñoz LM, et al. HMGB1 promotes recruitment of inflammatory cells to damaged tissues by forming a complex with CXCL12 and signaling via CXCR4. *J Exp Med* 2012; 209: 551–563.
62. Biscetti F, Ghirlanda G and Flex A. Therapeutic potential of high mobility group box-1 in ischemic injury and tissue regeneration. *Curr Vasc Pharmacol* 2011; 9: 677–681.
63. Feng L, Xue D, Chen E, et al. HMGB1 promotes the secretion of multiple cytokines and potentiates the osteogenic differentiation of mesenchymal stem cells through the Ras/MAPK signaling pathway. *Exp Ther Med* 2016; 12: 3941–3947.
64. Rossini A, Zacheo A, Mocini D, et al. HMGB1-stimulated human primary cardiac fibroblasts exert a paracrine action on human and murine cardiac stem cells. *J Mol Cell Cardiol* 2008; 44: 683–693.
65. Ranzato E, Patrone M, Mazzucco L, et al. Platelet lysate stimulates wound repair of HaCaT keratinocytes. *Br J Dermatol* 2008; 159: 537–545.